



## Validation of interannual simulations from the $1/8^\circ$ global Navy Coastal Ocean Model (NCOM)

A. Birol Kara <sup>\*</sup>, Charlie N. Barron, Paul J. Martin,  
Lucy F. Smedstad, Robert C. Rhodes

*Oceanography Division, Naval Research Laboratory, NRL Code 7320, Bldg., 1009, Stennis Space Center,  
MS 39529, United States*

Received 19 April 2004; received in revised form 15 December 2004; accepted 14 January 2005  
Available online 12 February 2005

---

### Abstract

A  $1/8^\circ$  global version of the Navy Coastal Ocean Model (NCOM) is used for simulation of upper-ocean quantities on interannual time scales. The model spans the global ocean from  $80^\circ\text{S}$  to a complete Arctic cap, and includes 19 terrain-following  $\sigma$ - and 21 fixed  $z$ -levels. The global NCOM assimilates three-dimensional (3D) temperature and salinity fields produced by the Modular Ocean Data Assimilation System (MODAS) which generates synthetic temperature and salinity profiles based on ocean surface observations. Model-data intercomparisons are performed to measure the effectiveness of NCOM in predicting upper-ocean quantities such as sea surface temperature (SST), sea surface salinity (SSS) and mixed layer depth (MLD). Subsurface temperature and salinity are evaluated as well. An extensive set of buoy observations is used for this validation. Where possible, the model validation is performed between year-long time series obtained from the model and time series from the buoys. The statistical analyses include the calculation of dimensionless skill scores (SS), which are positive if statistical skill is shown and equal to one for perfect SST simulations. Model SST comparisons with year-long SST time series from all 83 buoys give a median SS value of 0.82. Model subsurface temperature comparisons with the year-long subsurface temperature time series from 24 buoys showed that the model is able to predict temperatures down to 500 m reasonably well, with positive SS values ranging from 0.18 to 0.97. Intercomparisons of MLD reveal that the model

---

<sup>\*</sup> Corresponding author. Tel.: +1 228 688 5437.

*E-mail addresses:* [kara@nrlssc.navy.mil](mailto:kara@nrlssc.navy.mil) (A.B. Kara), [barron@nrlssc.navy.mil](mailto:barron@nrlssc.navy.mil) (C.N. Barron), [martin@nrlssc.navy.mil](mailto:martin@nrlssc.navy.mil) (P.J. Martin), [lsmedstad@nrlssc.navy.mil](mailto:lsmedstad@nrlssc.navy.mil) (L.F. Smedstad), [rhodes@nrlssc.navy.mil](mailto:rhodes@nrlssc.navy.mil) (R.C. Rhodes).

MLD is usually shallower than the buoy MLD by an average of about 15 m. Annual mean SSS and subsurface salinity biases between the model and buoy values are small. A comparison of SST between NCOM and a satellite-based Pathfinder data set demonstrates that the model has a root-mean-square (RMS) SST difference of 0.61 °C over the global ocean. Spatial variations of kinetic energy fields from NCOM show agree with historical observations. Based on these results, it is concluded that the global NCOM presented in this paper is able to predict upper-ocean quantities with reasonable accuracy for both coastal and open ocean locations.

Published by Elsevier Ltd.

*Keywords:* OGCM Validation; Buoy observations; Interannual simulation; SST; MLD; Optimal MLD; NCOM skill

---

## 1. Introduction

Model evaluation through model-data comparison studies is an important prerequisite of any quantitative ocean simulation. The major difficulty in such efforts has been a lack of global oceanic data sets of sufficient quality and duration to characterize the error statistics because observational data are relatively more sparse in the global ocean than in the atmosphere.

A potential source for the required observations are the mooring buoys located in different regions over the global ocean. These buoys have been reporting various upper ocean quantities on a regular basis. For example, the Tropical Atmosphere Ocean (TAO) array (McPhaden et al., 1998) has been reporting high resolution (e.g., hourly) sea surface temperature (SST), sea surface salinity (SSS), and subsurface temperature time series at various depth time series since 1986, and the National Oceanic Data Center (NODC) has also been measuring high resolution SST over coastal regions and open ocean stations since 1980s. With the availability these high quality data sets, SST and SSS simulations from ocean models can be validated in different regions of the global ocean. Availability of subsurface temperatures from the well-organized and maintained TAO array also allow calculation of mixed layer depth (MLD) on daily time scales to be used for validation of MLD simulations from ocean models.

Fine resolution satellite data sets (especially SST) present another observational basis for evaluation of ocean model performance over the global ocean. For example, The NOAA/NASA Pathfinder Advanced Very High Resolution Radiometer (AVHRR) SST product is a high quality data set derived from the NOAA polar orbiting series of satellites (e.g., Casey and Cornillon, 1999). This product represents a historical reprocessing of the entire AVHRR time series using consistent SST algorithms, improved satellite and inter-satellite calibration, quality control and cloud detection. It has a resolution of  $\approx 9$  km which is suitable for evaluating a fine resolution ocean model performance in predicting SST at various time scales over the global ocean.

In a companion paper (Barron et al., this issue), the  $1/8^\circ$  assimilative Navy Coastal Ocean Model (NCOM) is introduced with discussion of general model features, numerical formulation, global configuration, and the impact of vertical coordinate options. In this paper, we examine predictive capability of the global model as determined by comparisons with unassimilated observations during the validation test period. While the main focus of this paper is to examine model performance in representing upper ocean quantities, using buoy measurements over the global ocean on interannual time scales, other features of the model are validated and other

observational data sets are employed. All model validation is performed using unassimilated observations.

A global validation requires examination of model performance in as many places as possible by including both coastal and open ocean locations. In this paper, NCOM intercomparisons are performed using a set of statistical metrics and observations from many buoys selected in different regions of the global ocean. Variety in the buoy locations provides an excellent source for the model validation because there are buoys both in coastal and open ocean locations.

This paper is organized as follows: Section 2 gives a brief summary about NCOM numerics. Section 3 presents the atmospheric forcing and the assimilation scheme used in the model. Section 4 provides model-data comparisons obtained from the interannual simulations performed with high-resolution (6 hourly) atmospheric forcing. Finally, Section 5 covers the conclusions of this study.

## 2. NCOM description

The global NCOM used in this paper has a resolution of  $\approx 1/8^\circ$  latitude in mid-latitudes. The model has a free surface. It uses the primitive equations with the hydrostatic, Boussinesq, and incompressible approximations. The physics and numerics of NCOM are based largely on the Princeton Ocean Model (POM) as described in [Blumberg and Mellor \(1987\)](#), with some aspects from the Sigma/Z-level Model (SZM) ([Martin et al., 1998](#); [Martin, 2000](#)). The basic NCOM equations are in the Cartesian coordinate system, and details of these equations along with global model set up can be found in [Barron et al. \(this issue\)](#) and [Barron et al. \(2004\)](#). It is noted that the model equations themselves are defined according to a Cartesian coordinate system. These equations are implemented on a finite difference grid that is stretched spherical south of  $31^\circ\text{N}$  and rotated bipolar reprojected grid north of  $31^\circ\text{N}$ . There is no ice model in the simulations presented in this paper. Work on embedding the Polar Ice Prediction System (PIPS) 3.0, the latest generation of the Navy ice model, is underway for future versions of the model.

In this application, NCOM includes 19 terrain-following  $\sigma$ - and 21 fixed  $z$ -levels (a total of 40 material levels). The NCOM vertical grid uses  $\sigma$  coordinate from the surface down to a user-specified depth ( $z_s$ ) and  $z$ -levels below. Within the  $\sigma$  portion of the grid, each level is a fixed fraction of the total thickness occupied by the  $\sigma$  levels, as in POM. In the  $z$ -level portion of the grid, bottom depth is rounded the nearest  $z$ -level. In general, the use of combined  $\sigma$  and  $z$  level coordinates in a single ocean model provides some flexibility in grid configuration. For example,  $\sigma$  coordinates in the upper levels improve resolution of changes in sea surface elevation and enhance representation of vertical shear and bottom depth in shallow regions. Using  $z$ -levels below  $z_s$  avoids the problems associated with  $\sigma$ -levels in regions of steep topography and limits the combined thickness of all  $\sigma$ -levels. Since each  $\sigma$ -level is a fixed fraction of the  $\sigma$  total, the underlying  $z$ -levels enable NCOM to maintain consistent high resolution near the surface in deep-water regions. The vertical coordinate is logarithmically stretched to focus resolution near the surface with a maximum rest surface level thickness of 1 m.

NCOM surface boundary conditions are the surface stress for the momentum equations, the surface heat flux for the temperature equation, and the effective surface salt flux for the salinity equation. The bottom boundary conditions are the bottom drag for the momentum equations,

which is parameterized by a quadratic drag law, and zero flux for the temperature and salinity equations. The model equations are solved on an Arakawa C grid and the horizontal grid is orthogonal curvilinear as in POM (Blumberg and Herring, 1987).

### 3. Atmospheric forcing and data assimilation

Global NCOM uses atmospheric forcing from the Navy Operational Global Atmospheric Prediction System (NOGAPS). The main features of the NOGAPS forcing are described in Hogan and Rosmond (1991), and recent improvements along with changes to the system are provided in Rosmond et al. (2002). NOGAPS provides relatively high frequency atmospheric forcing, in particular important for the ocean mixed layer where inertial oscillations are excited by transient forcing from surface winds. The NOGAPS fluxes are output at 6 hourly intervals to support this requirement. The interannual NCOM simulations presented here are performed using high-resolution wind forcing (pseudo-wind stresses) and thermal forcing (shortwave and longwave radiation entering the sea) obtained from the NOGAPS. There is no precipitation field used in the model due to uncertainties in the NOGAPS precipitation fields. The sensible and latent heat fluxes are calculated every time step using the model SST in bulk formulations (Kara et al., 2002).

NCOM assimilates temperature and salinity fields produced by the Modular Ocean Data Analysis System (MODAS) developed at the NRL (Fox et al., 2002a). MODAS consists of a collection of over 200 programs and utilities for combining irregularly sampled remote-sensed data and in situ measurements to create 3D estimates of temperature and salinity over the global ocean. MODAS performs quality checking and optimum interpolation of ocean observations (Bretherton et al., 1976), including temperature, salinity, and sea surface height (SSH). The SSH and SST are gridded by optimum interpolation using altimeter (Jacobs et al., 2002) and multi-channel SST (MCSST) products from the Naval Oceanographic Office (NAVOCEANO) (Fox et al., 2002b). The MCSST data are obtained from multiple 5-channel AVHRR whose calibration is explained in Brown et al. (1993). For the fields it prepares for global NCOM, MODAS uses SSH from the assimilative  $1/16^\circ$  global Naval Research Laboratory Layered Ocean Model (NLOM), a US Navy operational product (Smedstad et al., 2003). Detailed description and simulation capabilities of NLOM are given in Wallcraft et al. (2003), Kara et al. (2003a) and Kara et al. (2004). NLOM SSH rather than MODAS 2D SSH is used to take advantage of the improved nowcast skill of the NLOM dynamics over the MODAS statistical model and the ability of NLOM to better quantify the steric component of its SSH.

Data preparation for assimilation to NCOM begins with SST from MODAS 2D and SSH from NLOM. Subtracting the NLOM climatological mean SSH from daily SSH yields an SSH deviation, which is passed along with MODAS 2D SST to the MODAS dynamic climatology module for calculation of synthetic temperature and salinity profiles. At this stage, available in situ observations can be assimilated into the 3D analyses. For the present study, no in situ data have been included, so that these may be used for independent validation. After converting temperature to potential temperature, the 3D potential temperature and salinity fields are interpolated to the model grid.

Data assimilation used in NCOM is done using two mechanisms: (1) adjustment of surface heat and salinity fluxes, and (2) insertion of subsurface temperature and salinity profiles. In both cases,

the strength of assimilation is controlled by a gridded weighting function that reflects the relative confidence between the model and the data. Presently this is specified and fixed; ongoing efforts to improve the data assimilation include using the analysis and background model errors to provide a more appropriate weighting. The slow data insertion technique allows the model to incrementally adjust to the data with minimal dynamic disruption (Rhodes et al., 2002). Preparation of the data fields is independent of the NCOM assimilation itself, allowing the model to accommodate a variety of approaches to preparing the observational analyses.

Using the high-resolution atmospheric forcing fields from the NOGAPS along with the assimilation scheme presented above, global NCOM was run to examine model performance in predicting upper ocean quantities. The model intercomparisons are presented in Section 4.

#### 4. Model-data comparisons

Model-data comparisons are first conducted to evaluate  $1/8^\circ$ NCOM performance in predicting SST over the global ocean. Using the daily SST values from the model, an annual mean field is formed over 2002. The model uses wind and thermal forcing from NOGAPS, and relaxes to MODAS synthetic temperature and salinity derived from  $1/8^\circ$  MODAS2D SST and  $1/16^\circ$  NLOM SSH as explained in Section 3. The annual mean model SST are shown for Atlantic, Pacific and Indian Oceans, separately (Fig. 1a).

Similar to mean values, SST standard deviation is also calculated at each model grid point to reveal regions of relatively high and low SST variability in 2001 (Fig. 1b). The SST standard deviation values are relative to the mean SST in 2001. As expected, there are relatively large variability (e.g.,  $>3.0^\circ$ ) due to SST seasonal cycle, and SST variability is generally small ( $<0.5^\circ$ ) in the western equatorial Pacific warm pool, indicating that NCOM is producing the expected large-scale variability patterns. For more quantitative evaluations, SST standard deviations are  $0.43$  and  $0.67^\circ\text{C}$  at ( $2^\circ\text{N}$ ,  $156^\circ\text{E}$ ), and ( $2^\circ\text{N}$ ,  $165^\circ\text{E}$ ), respectively as calculated from daily SST time series from two buoys (McPhaden et al., 1998) located in the Equatorial Pacific in 2001. The corresponding NCOM standard deviation values are  $0.45$  and  $0.73^\circ\text{C}$  at the same locations, demonstrating the model's success in predicting daily SST variability.

NCOM SSTs are now compared with SSTs obtained from the interannual Pathfinder data set (Casey and Cornillon, 1999, 2001) across the global domain (Fig. 1c). The purpose for this comparison is to examine overall model performance in 2001. Data gaps in this satellite-based data set may occur primarily due to cloud cover because of the inability of the infrared sensor to detect ocean temperatures in these conditions. The Pathfinder SST is based directly on satellite data, so it is treated as the "truth" in model-data comparisons. The accuracy of the Pathfinder SST is  $\approx 0.3$ – $0.5^\circ\text{C}$  based on several studies (Kearns et al., 2000; D'Ortenzio et al., 2001; Casey and Cornillon, 2001). The Pathfinder SST has equal-angle grids of 4096 pixels/360 degrees (nominally referred to as the 9 km resolution) over the global ocean. This grid resolution is also very close to that of global NCOM, making the Pathfinder SST an ideal candidate for evaluation of model results.

It is noted that there are also coarse resolution Pathfinder SST data sets ( $\approx 18$  and  $54$  km) but they were not used for NCOM validation because the use of an SST data set consistent with the model resolution ( $\approx 9$  km) is an optimal choice. The Pathfinder SST mean is created by averaging

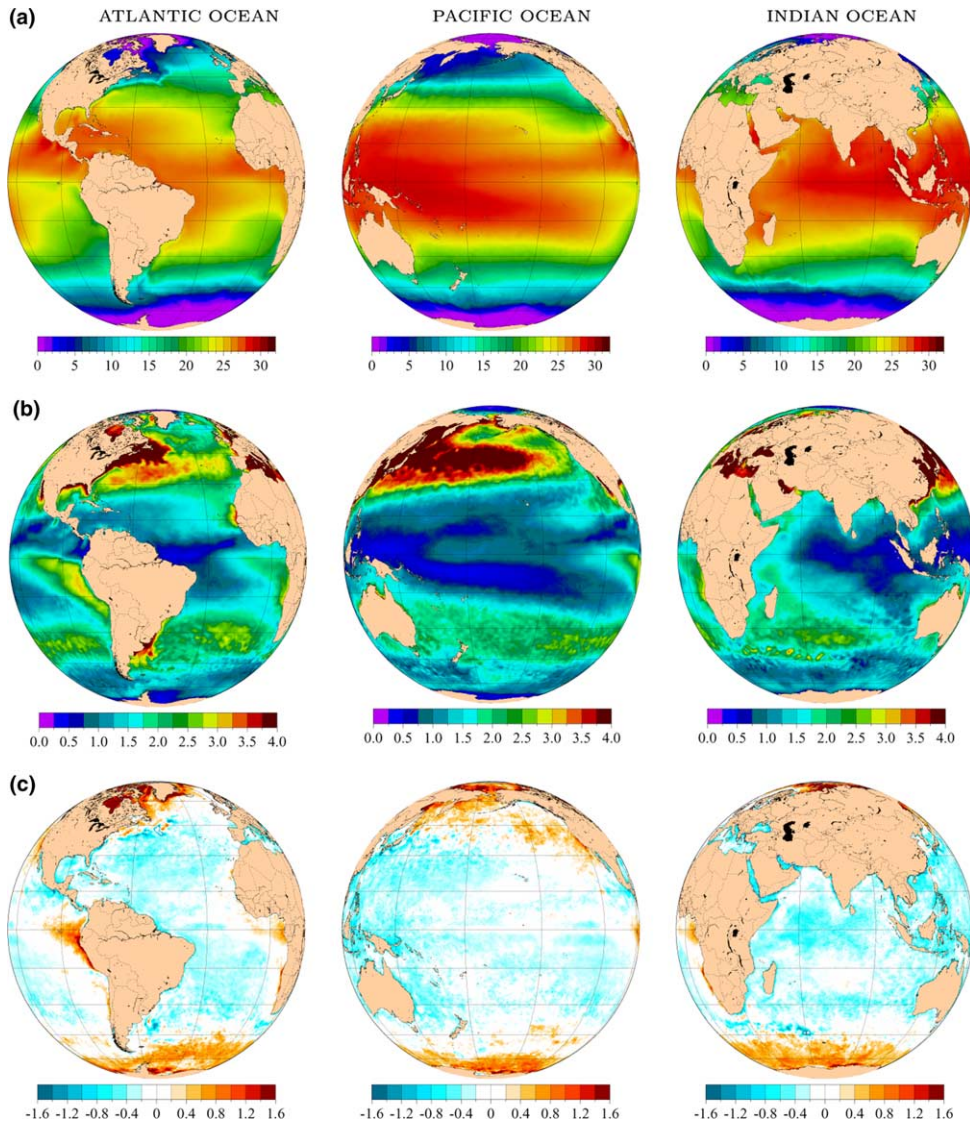


Fig. 1. Global SST analysis obtained from the  $1/8^\circ$  assimilative NCOM over the global ocean in 2001: (a) annual mean SST from the model, (b) the model SST standard deviation, and (c) annual mean of monthly SST difference between the model and Pathfinder. Note that the Pathfinder SST is interpolated on the NCOM grid, and all fields are constructed using daily SSTs at each model grid point.

daily fields into monthly means. Both daytime and nighttime daily fields are included in each monthly average (Casey and Cornillon, 1999). A  $7 \times 7$  median filter is applied to fill in many of the gaps, and a  $7 \times 7$  median smoother is used over the entire field to remove small-scale noise.

To prepare model-data comparisons at each model grid point, the annual mean NCOM SST are linearly interpolated to the original Pathfinder SST grid. The model SST evaluations are

performed only at grid points where the Pathfinder SST are available. Missing SST values in the Pathfinder SST are generally at high latitudes in 2001 (not shown).

The difference between NCOM and the Pathfinder SST (Fig. 1c) demonstrates that annual mean NCOM SST bias is usually small, with values between  $-0.4\text{ }^{\circ}\text{C}$  and  $0.4\text{ }^{\circ}\text{C}$  over the most of the global ocean in 2001. Note that there are many regions where SST difference is extremely small ( $\pm 0.2\text{ }^{\circ}\text{C}$ ) as shown with white in color in the figure. The global average of the SST bias and RMS difference between the annual mean NCOM and Pathfinder SSTs are  $0.11\text{ }^{\circ}\text{C}$  and  $0.61\text{ }^{\circ}\text{C}$ , respectively. These values are based on the statistics calculated at 2497574 model grid points.

Overall, there are more regions of NCOM SST having a cooler mean than that of the Pathfinder data. The annual mean model SST is cooler by about  $1\text{ }^{\circ}\text{C}$  in the North Pacific Ocean where the Kuroshio current system is located, and in the North Atlantic Ocean where the Gulf Stream is located and in some regions of the Southern Ocean. The NCOM SST is warmer in the polar regions and near western coasts. The smallest differences occur in the central areas of the three basins. In summary, given that the accuracy of the Pathfinder SST is  $0.3\text{--}0.5\text{ }^{\circ}\text{C}$ , we can indicate that the NCOM SST errors are within the Pathfinder SST accuracy (i.e.,  $<0.5\text{ }^{\circ}\text{C}$ ) in open ocean, along continental boundaries and the equatorial upwelling region. This demonstrates the success of the  $1/8^{\circ}$  assimilative NCOM in representing SST over the global ocean.

Regional kinetic energy fields from NCOM are tools for locating major currents and are validated using IR fronts. Spatial variation of annual mean surface kinetic energy and annual mean surface eddy kinetic energy fields from NCOM are shown in Fig. 2 for the Gulf Stream and the Kuroshio region in 2001. For comparison, 2001 mean NAVOCEANO front boguses (white in color), determined from infrared imagery (IR), are superimposed in these figures. Both the model values and the IR fronts are formed using daily means over the 365-day period. The kinetic energy

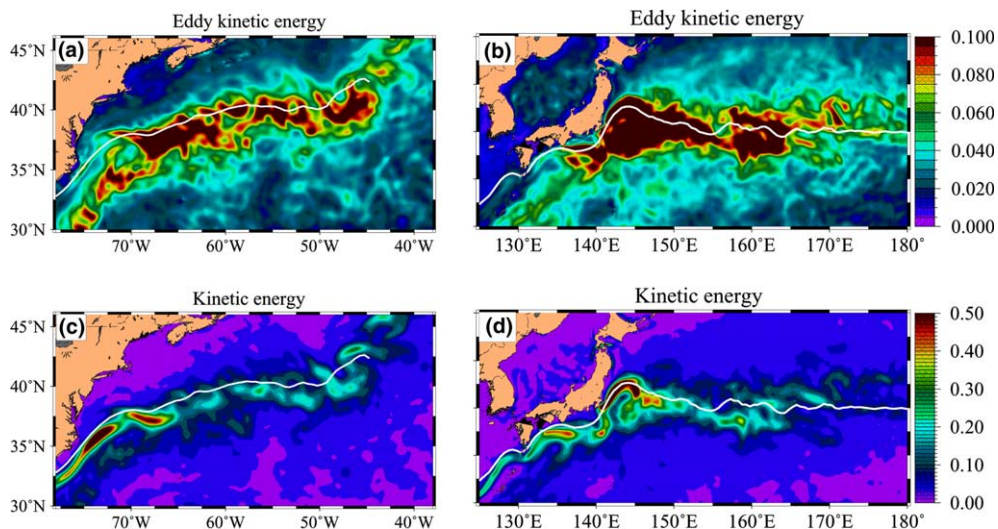


Fig. 2. Spatial variations of mean surface eddy kinetic energy ( $\text{m}^2 \text{s}^{-2}$ ) and mean surface kinetic energy ( $\text{m}^2 \text{s}^{-2}$ ) obtained from NCOM simulations for the Kuroshio and Gulf Stream locations in 2001. The mean fields were formed during one year period from 01 January 2001 to 31 December 2001. Note that front boguses from the NAVOCEANO IR is shown in white in color.

fields indicate good agreement between the northern edge of the current core in the model and the mean boundaries of the Kuroshio and Gulf Stream as determined by independent NAVOCEANO northwall boguses. The NAVOCEANO IR fronts are associated with high kinetic energy in the model.

Upper ocean quantities from NCOM are also validated using buoy observations reported from three sources: (1) the Tropical Atmosphere–Ocean (TAO) array (McPhaden et al., 1998), (2) the Pilot Research Moored Array (PIRATA) (Servain et al., 1998), and (3) the National Oceanic Data Center (NODC) database (<http://www.nodc.noaa.gov/BUOY/buoy.html>). Fig. 3 shows locations of these buoy observations for year 2001.

The TAO array, located in the equatorial Pacific Ocean, consists of approximately 70 buoys between 8°S–8°N and 137°E–95°W. The PIRATA is an array of 12 buoys in the Tropical Atlantic, and they are very sparse in comparison to the TAO buoys. The NODC database holds different types of buoy observations collected by the National Data Buoy Center (NDBC), and these buoys are located at the Gulf of Mexico, Northwest/Southwest US coast, Great Lakes, Hawaii and Alaska coasts. Because NCOM does not assimilate any buoy data, validating model results using buoy observations from TAO, PIRATA, and NODC serves as an independent verification.

All the buoys include different upper ocean quantities (Table 1). These buoy observations (or calculated quantities) include daily-averaged time series of SST, SSS, MLD, subsurface temperatures, and subsurface salinities. The TAO and PIRATA buoys do not directly report MLD, but they provide subsurface temperatures measured at several depths down to 500 m from which MLD can be calculated. There were no subsurface temperature time series available from the NODC buoys. Therefore, no MLD time series from the NODC buoys are used for the NCOM intercomparisons. We only use time series that do not have a lot of data voids. When a few data voids were found in the time series, they are filled in using linear interpolation. Overall, a total of 164 year-long daily time series of upper ocean quantities were prepared for the NCOM intercomparisons.

Several statistical metrics are used for comparing the time series (e.g., SST, MLD, and subsurface temperatures) predicted by the model (NCOM) with the time series from the buoys. A brief summary of these metrics is given here. Let  $X_i$  ( $i = 1, 2, \dots, n$ ) be the set of  $n$  buoy (i.e., reference) values, and let  $Y_i$  ( $i = 1, 2, \dots, n$ ) be the set of corresponding NCOM estimates. Also let  $\bar{X}$  ( $\bar{Y}$ ) and  $\sigma_X$  ( $\sigma_Y$ ) be the mean and standard deviations of the reference (estimate) values, respectively. Given this information, the statistical metrics (e.g., Murphy, 1988) between the buoy and the model time series can be expressed as follows:

$$ME = \bar{Y} - \bar{X}, \quad (1)$$

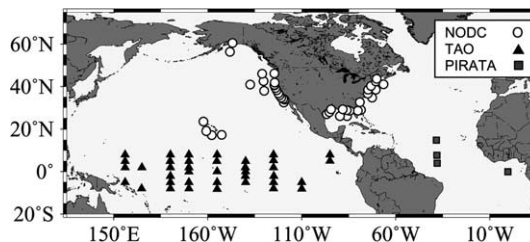


Fig. 3. Locations of NODC, PIRATA and TAO used for model-data comparisons in 2001.



Table 1

Availability of observed upper ocean variables used for assessing the interannually forced NCOM in 2001

| Daily buoy observation | Buoy source | Year-long time series |
|------------------------|-------------|-----------------------|
| SST                    | NODC        | 41                    |
| SST                    | TAO         | 38                    |
| SST                    | PIRATA      | 4                     |
| SSS                    | TAO         | 11                    |
| SSS                    | PIRATA      | 2                     |
| $T_{\text{sub}}$       | TAO         | 21                    |
| $T_{\text{sub}}$       | PIRATA      | 3                     |
| $S_{\text{sub}}$       | TAO         | 7                     |
| $S_{\text{sub}}$       | PIRATA      | 13                    |
| MLD                    | TAO         | 21                    |
| MLD                    | PIRATA      | 3                     |

All buoy observations (or calculated quantities, such as MLD) are daily time series. The total number of available daily year-long time series data used for NCOM intercomparisons throughout the paper is also given along with the source of time series.

$$\text{RMSD} = \left[ \frac{1}{n} \sum_{i=1}^n (Y_i - X_i)^2 \right]^{1/2}, \quad (2)$$

$$R = \frac{1}{n} \sum_{i=1}^n (X_i - \bar{X})(Y_i - \bar{Y}) / (\sigma_X \sigma_Y), \quad (3)$$

$$\text{SS} = R^2 - \underbrace{[R - (\sigma_Y / \sigma_X)]^2}_{B_{\text{cond}}} - \underbrace{[(\bar{Y} - \bar{X}) \sigma_X]^2}_{B_{\text{uncond}}}, \quad (4)$$

where ME is the bias or annual mean difference, RMSD is the root-mean-square difference,  $R$  is the correlation coefficient, and SS is the skill score. All the model-data comparisons are performed in 2001, so  $n$  is 365. Note from (4) that  $R^2$  is equal to SS only when  $B_{\text{cond}}$  and  $B_{\text{uncond}}$  are zero. Because these two biases are never negative, the  $R$  value can be considered to be a measure of “potential” skill (Stewart, 1990), i.e., the skill that one can obtain by eliminating bias from the model results. The SS is 1.0 for perfect NCOM simulations, and can be negative if the NCOM simulation has normalized amplitudes larger than the correlation or large biases in the mean (Murphy and Epstein, 1989). The reader is also referred to Kara et al. (2003a) for an extensive application of the same statistical metrics used for validating a global ocean model.

#### 4.1. SST

A set of 81 moored buoys is used for the NCOM SST intercomparisons in 2001. These include 38 TAO buoys, 4 PIRATA buoys and 41 NODC buoys located in different regions of the global ocean (see Appendix A). There are buoys located in relatively shallow coastal locations (most of the NODC buoys) and in the open ocean (the TAO, PIRATA, and a few of the NODC buoys). All the buoys report hourly SST measured at a depth of  $\approx 1$  m below the sea surface.

An assessment of instrumental accuracies indicates errors of about  $0.03\text{ }^{\circ}\text{C}$  for buoy SST (Freitag et al., 1994).

For the model-data comparisons, daily-averaged buoy SSTs were formed. No smoothing was applied to the original values. Daily-averaged SSTs from NCOM were also extracted at the buoy locations. Here the reader is informed that the average latitude/longitude positions of the buoys are used to extract SST from the model grid because buoy locations can change from day to day, and they may also change by a few km whenever a mooring is recovered and a new one redeployed. In particular, positions of moored buoys can change over the course of a few days to a week depending on the current regime by up to 2 nautical miles. This is a diameter within which the buoy moves. Since each mooring moves in time and space from its deployment position, we calculated average position based on the historical latitude and longitude data for each buoy. While the model validation presented here are based only on comparisons with buoys in 2001, using the historical average of latitude and longitude location provides a consistent coordinate at each buoy when the model validation would possibly be extended to earlier or later years. Thus, NCOM SST was extracted using the average latitude and longitude values for each buoy. For ease of notation, nearest integer values of average latitude and longitude is used for each buoy in the tables shown in [Appendix A](#) and throughout the text.

As mentioned previously,  $1/8^{\circ}$ NCOM used in this paper assimilates  $1/8^{\circ}$  MODAS SST analysis of satellite IR data whose details are given in Section 3. Therefore, the model-data comparisons presented here also include the MODAS SST. Including the MODAS SST in the validation allows us to measure the effectiveness of the assimilation procedure in the model.

As examples to illustrate the model assessment procedure used throughout the paper, detailed model-data comparison results are shown for four buoy locations. These buoys are chosen to represent different regions over the global ocean: a coastal NODC buoy in the Gulf of Mexico ( $29^{\circ}\text{N}$ ,  $085^{\circ}\text{W}$ ), an open ocean TAO buoy in the eastern equatorial Pacific Ocean ( $2^{\circ}\text{N}$ ,  $125^{\circ}\text{W}$ ), a PIRATA buoy in the tropical Atlantic Ocean ( $15^{\circ}\text{N}$ ,  $038^{\circ}\text{W}$ ), and a high latitude NODC buoy in the north Pacific Ocean ( $61^{\circ}\text{N}$ ,  $147^{\circ}\text{W}$ ). [Fig. 4](#) shows daily SST time series from the buoy observations, NCOM, and MODAS during 2001. NCOM is able to simulate the daily SST variability quite well at all these locations. [Table 2](#) shows statistical model-data comparisons between the buoy and NCOM SST time series at these four locations during 2001. Statistical results for MODAS vs. NCOM SST time series and buoy vs. MODAS SST time series are also included. The latter is included because NCOM assimilates MODAS SST and we would like to determine its accuracy with respect to the buoy values. Overall, the ME values (i.e., the annual mean SST bias) and the RMSD values are very small between the NCOM predicted SSTs and the buoy SSTs. The model success is also evident from the large and positive SS values, indicating that NCOM is able to simulate SST with an acceptable accuracy. It is not surprising that the statistical results between MODAS and NCOM are slightly better than the results between the buoys and NCOM because the model simulation includes MODAS SST assimilation; for these results no buoy SSTs are assimilated in either MODAS or NCOM.

Note that the RMSD value of  $0.86\text{ }^{\circ}\text{C}$  between the buoy and NCOM SSTs at ( $61^{\circ}\text{N}$ ,  $147^{\circ}\text{W}$ ) is almost twice as much as the value of  $0.42\text{ }^{\circ}\text{C}$  at ( $15^{\circ}\text{N}$ ,  $038^{\circ}\text{W}$ ), which might seem to indicate that the NCOM SST simulation at the latter buoy is better than at the former one. However, an examination of the dimensionless SS values reveals that the SS value of 0.95 at ( $61^{\circ}\text{N}$ ,  $147^{\circ}\text{W}$ ) is very large; while, there is almost no model skill at ( $15^{\circ}\text{N}$ ,  $038^{\circ}\text{W}$ ). This is due to the fact that

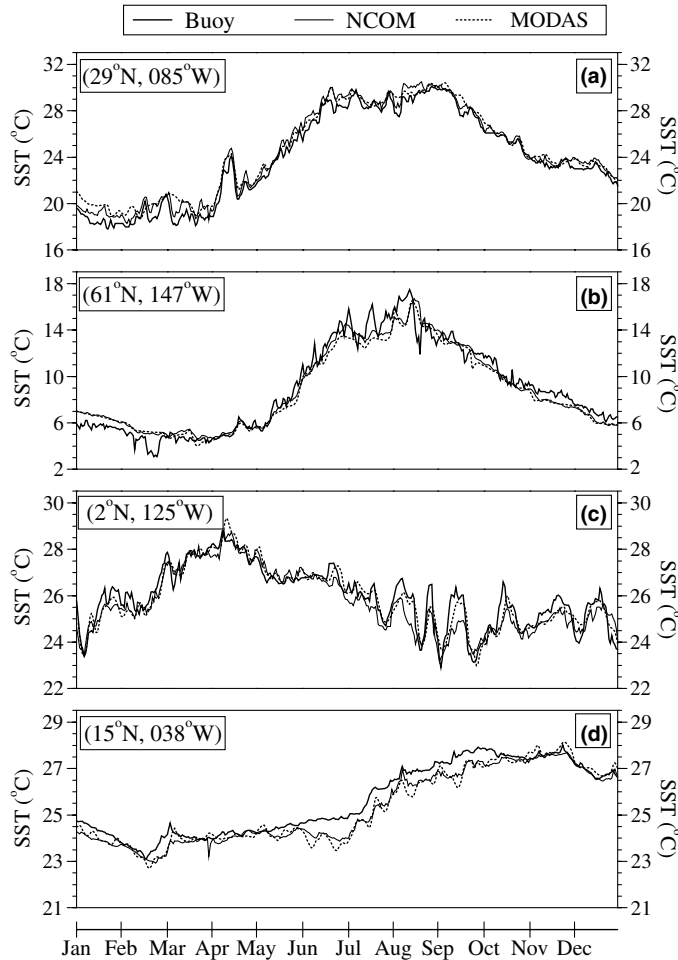


Fig. 4. Daily SST time series obtained from buoy, NCOM and MODAS at four locations in 2001: (a) an NODC buoy ( $29^{\circ}\text{N}$ ,  $085^{\circ}\text{W}$ ), (b) a NODC buoy ( $61^{\circ}\text{N}$ ,  $147^{\circ}\text{W}$ ), (c) a TAO buoy ( $2^{\circ}\text{N}$ ,  $125^{\circ}\text{W}$ ) and (d) a PIRATA buoy ( $15^{\circ}\text{N}$ ,  $038^{\circ}\text{W}$ ). Note that global NCOM assimilates  $1/8^{\circ}$  MODAS SST analysis of satellite IR data. The  $x$ -axis is labeled starting from the beginning of each month.

the standard deviation of the buoy SST ( $3.82^{\circ}\text{C}$ ) at the high latitude NODC buoy is greater than that of the buoy SST ( $0.42^{\circ}\text{C}$ ) at the buoy located in the equatorial Atlantic Ocean. Thus, the dimensionless SS analysis serves as a clear distinction between the two locations, which illustrates that using only one statistical metric (e.g., RMSD) is not enough to decide whether or not the model is performing well.

The model-data comparisons shown in Table 2 are extended to all the TAO, PIRATA, and NODC buoys (see Appendix A). In other words, RMSD, ME,  $R$ , and SS values (buoy vs. NCOM, MODAS vs. NCOM, and buoy vs. MODAS) are calculated at each buoy location, so that the overall NCOM performance in predicting SST can be assessed in 2001. This yields a total of 83 year-long daily SST time series. Combining each set of statistics under one

Table 2

Statistical verification of daily SST time series between buoy vs. NCOM, buoy vs. MODAS and MODAS vs. NCOM at four different buoy locations chosen at open ocean and coastal regions to represent different regions of the global ocean

|                       | RMSD (°C) | ME (°C) | $\sigma_X$ (°C) | $\sigma_Y$ (°C) | $R$  | SS   |
|-----------------------|-----------|---------|-----------------|-----------------|------|------|
| <b>Buoy vs. NCOM</b>  |           |         |                 |                 |      |      |
| (29°N, 085°W)         | 0.65      | 0.52    | 3.92            | 3.85            | 1.00 | 0.97 |
| (61°N, 147°W)         | 0.86      | −0.09   | 3.82            | 3.52            | 0.98 | 0.95 |
| (2°N, 125°W)          | 0.56      | −0.25   | 1.27            | 1.30            | 0.92 | 0.81 |
| (15°N, 038°W)         | 0.42      | −0.27   | 0.42            | 0.62            | 0.87 | 0.00 |
| <b>Buoy vs. MODAS</b> |           |         |                 |                 |      |      |
| (29°N, 085°W)         | 0.80      | 0.58    | 3.92            | 3.70            | 0.99 | 0.96 |
| (61°N, 147°W)         | 0.94      | −0.26   | 3.82            | 3.41            | 0.98 | 0.94 |
| (2°N, 125°W)          | 0.38      | −0.09   | 1.27            | 1.31            | 0.96 | 0.91 |
| (15°N, 038°W)         | 0.37      | −0.16   | 0.42            | 0.64            | 0.88 | 0.22 |
| <b>MODAS vs. NCOM</b> |           |         |                 |                 |      |      |
| (29°N, 085°W)         | 0.47      | −0.06   | 3.70            | 3.85            | 0.99 | 0.98 |
| (61°N, 147°W)         | 0.35      | 0.18    | 3.41            | 3.52            | 1.00 | 0.99 |
| (02°N, 125°W)         | 0.38      | −0.16   | 1.31            | 1.30            | 0.97 | 0.92 |
| (15°N, 038°W)         | 0.21      | −0.11   | 0.64            | 0.62            | 0.96 | 0.89 |

Comparisons are made in 2001, using variety of statistical metrics as described in the text. Statistics includes root-mean-square difference (RMSD), mean error (ME), standard deviation ( $\sigma_X$  for buoy or MODAS and  $\sigma_Y$  for NCOM), correlation coefficient ( $R$ ), and skill score (SS), all of which are explained in Section 4 in the text. The number of cases is 365 for each category, and SS values close to 1 indicates perfect simulations. Note that global NCOM assimilates 1/8° MODAS SST analysis of satellite IR data.

category, we then calculate the cumulative frequency of ME, RMSD,  $R$ , and SS to obtain modal (median) statistics. Error statistics between the buoy observations and NCOM simulations for 83 year-long daily time series give median ME of 0.09 °C, RMSD of 0.44 °C,  $R$  of 0.94, and SS of 0.82. Similar median statistics between the buoy data and the MODAS SST time series gives median ME of 0.07 °C, RMSD of 0.45 °C,  $R$  of 0.94, and SS of 0.82. It is noted that the overall agreement between the pairs of buoy vs. NCOM SSTs and buoy vs. MODAS SSTs is almost identical, which further indicates the model bias towards the MODAS SST. Finally, we note that the agreement between MODAS and NCOM is highest, giving a median ME of −0.05 °C, RMSD of 0.30 °C,  $R$  of 0.97, and SS of 0.92. This is due to assimilation of MODAS SST by NCOM.

#### 4.2. Subsurface temperatures

Unlike the NODC buoys, both TAO and PIRATA buoys report subsurface temperatures measured at various depths from surface down to 500 m. The buoys reporting subsurface temperatures can be considered under two categories based on the water depths at which subsurface measurements are taken (Table 3). There are a total of 24 buoys used for NCOM subsurface temperature validation that have nearly complete data in 2001. An assessment of instrumental accuracies indicates about 0.1 °C for subsurface temperature (Freitag et al., 1994). Similar to SST, a few missing values were filled using a linear interpolation.

Table 3

A list of daily subsurface temperature availability from TAO and PIRATA buoys used for validating NCOM subsurface temperatures in 2001

| Set I  |               | Set II |              |
|--------|---------------|--------|--------------|
| Buoy   | Location      | Buoy   | Location     |
| PIRATA | (15°N, 038°W) | TAO    | (2°N, 170°W) |
| TAO    | (2°S, 125°W)  | TAO    | (2°N, 180°W) |
| TAO    | (2°S, 140°W)  | TAO    | (2°S, 180°W) |
| TAO    | (5°N, 110°W)  | TAO    | (5°N, 180°W) |
| TAO    | (5°N, 125°W)  | TAO    | (5°S, 155°W) |
| TAO    | (5°N, 140°W)  | TAO    | (5°S, 170°W) |
| TAO    | (5°S, 110°W)  | TAO    | (5°S, 180°W) |
| TAO    | (5°S, 125°W)  | TAO    | (8°N, 170°W) |
| PIRATA | (6°S, 010°W)  | TAO    | (8°N, 180°W) |
| PIRATA | (8°N, 038°W)  | TAO    | (8°S, 155°W) |
| TAO    | (8°N, 095°W)  | TAO    | (8°S, 165°E) |
| TAO    | (8°N, 125°W)  | TAP    | (8°S, 170°W) |

For model-data comparisons, no smoothing is applied to buoy subsurface temperatures, and NCOM subsurface temperatures are also extracted at the depths consistent with the ones provided in set I and set II (see Table 3) at each buoy location. Also included are 1/8° MODAS subsurface temperatures and climatological MODAS subsurface temperatures because NCOM assimilates MODAS subsurface temperatures. Neither MODAS nor NCOM assimilated any buoy subsurface temperatures.

As an example, daily subsurface temperatures from NCOM are compared to those from buoy, MODAS and MODAS climatology at (2°N, 170°W), a TAO buoy from set II located near the central equatorial Atlantic Ocean (Fig. 5). Close agreement between the NCOM and buoy subsurface temperatures is evident, especially near the surface and below 200 m. To obtain error statistics at each depth level, statistical metrics were calculated using the year-long daily temperature time series at 1, 20, 40, 60, 80, 100, 120, 140, 180, 300, and 500 m, separately. For all the comparisons, the buoy temperatures are taken as reference values; in other words, the NCOM, MODAS, and climatological subsurface temperatures are compared to the buoy subsurface temperatures (Fig. 6). Results indicate that NCOM has equal or lower RMSD than MODAS down to 500 m. Both NCOM and MODAS are superior to climatology for depths shallower than 250 m.

The analysis procedure used for the TAO buoy at (2°N, 170°W) is repeated for each buoy shown in Table 3, so that summary statistics including all buoys can be obtained. Statistical values are calculated for set I and set II buoys, separately. The reason for this is that the water depths at which the subsurface temperatures were taken are different for both sets as mentioned before. It should also be noted that summary statistics, for example averaged RMSD value at 20 m, are calculated using temperatures at 20 m from all buoys (i.e., 12 year-long daily time series for the buoys, NCOM, MODAS, and climatology) rather than averaging RMSD values at 20 m calculated from each individual buoy, separately. Summary statistics for the set I and set II buoys are shown in Fig. 7. In general, both NCOM and MODAS have lower RMSD values than climatology, which indicates some model skill. However, MODAS and NCOM have low skill in

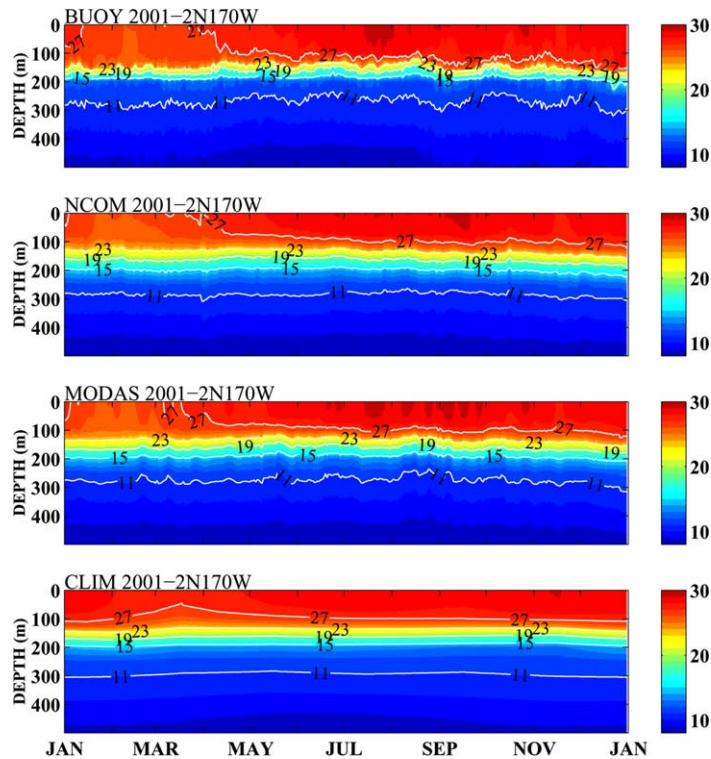


Fig. 5. Spatial daily subsurface temperature variability ( $^{\circ}\text{C}$ ) obtained from buoy, NCOM and MODAS and MODAS climatology at a TAO buoy, ( $2^{\circ}\text{N}$ ,  $170^{\circ}\text{W}$ ), located in the equatorial Pacific Ocean. All are in 2001, and the water depths at which buoy subsurface measurements were taken are at 1, 25, 50, 75, 100, 125, 150, 200, 250, 300, and 500 m. Accuracy of subsurface temperatures reported from the buoy is  $0.03^{\circ}\text{C}$ . Note that global NCOM assimilates  $1/8^{\circ}$  MODAS subsurface temperatures. The  $x$ -axis is labeled starting from the beginning of each month.

predicting subsurface temperatures between 100 and 150 m. One of the reasons for this low skill is that the MODAS subsurface temperatures show a bias relative to the buoy temperatures at these depths.

#### 4.3. MLD

In this section surface ocean layer depth comparisons are performed at all buoy locations used in Section 4b. Surface ocean layer depth can be calculated at these buoy locations because subsurface temperatures from buoy, NCOM, MODAS and MODAS climatology are available. There are two commonly used surface ocean layer depth definitions: (1) an isothermal layer depth (ILD), and (2) an isopycnal layer depth (MLD). The methodology for inferring the ILD and MLD used in this paper is fully described by Kara et al. (2000a), showing that MLD is best defined using a variable density definition. In brief, the ILD [MLD] can be summarized in its simplest form as being the depth at the base of an isothermal [isopycnal] layer, where the temperature [density] has changed by a variable value of  $\Delta T$  [ $\Delta\sigma_t$ ] from the temperature [density] at a reference

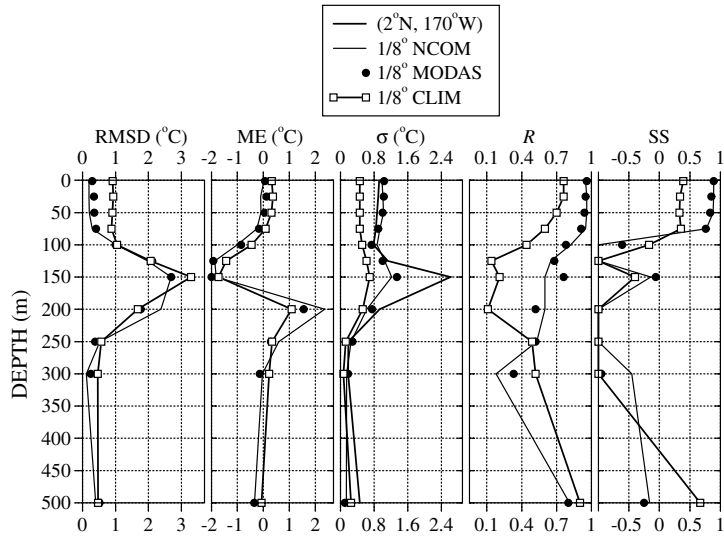


Fig. 6. Variations of RMSD, ME,  $\sigma$ ,  $R$  and SS values with depth from surface to 500 m below the sea surface at ( $2^{\circ}\text{N}$ ,  $170^{\circ}\text{W}$ ) located in the equatorial Pacific Ocean. All statistical results are obtained with respect to 365 daily-averaged buoy values in 2001. They are shown for NCOM, MODAS and MODAS climatology.

depth of 10 m. For the isopycnal layer this means  $\Delta\sigma_t = \sigma_t(T + \Delta T, S, P) - \sigma_t(T, S, P)$ , where  $P$  is set to zero. Density is usually calculated using an equation of state with no pressure dependence (Millero et al., 1980; Millero and Poisson, 1981).

While daily salinity values from NCOM, MODAS and MODAS climatology are available at the buoy locations in 2001, daily salinity measurements from buoys were not available. To be consistent with all products, we calculate true surface ocean layer depth based on the ILD definition (temperature-based) rather than MLD definition (density-based via salinity). It is noted that specific attention needs to be given to calculation of layer depth, especially in the equatorial Pacific due to existence of barrier layers as explained by Kara et al. (2000b). Although, the ILD definition with a  $\Delta T$  value of  $0.5^{\circ}\text{C}$  is approximately equal to optimal MLD at the equatorial ocean, this constant value can be quite variable from one location to another (Kara et al., 2003b). Thus, we use a location-specific  $\Delta T$  value determined at each buoy obtained from the annual mean  $\Delta T$  map of Kara et al. (2003b). This annual mean field provides spatial variation of  $\Delta T$  values at each  $1^{\circ} \times 1^{\circ}$  grid, allowing us to obtain an ILD that is equivalent to the optimal MLD at each buoy location.

Fig. 8 shows daily optimal MLD variability calculated from the buoy as well as the ones calculated from NCOM, MODAS and MODAS climatology. MLD varies considerably from one day to the next. Overall, there is not a significant underestimation or overestimation of buoy MLD by the model. Although NCOM assimilates synthetic temperature and salinity profiles from MODAS, NCOM is in closer agreement than MODAS to the observed MLD (see also Fig. 9). This also demonstrates that the model is superior to MODAS in estimating MLD variability at ( $5^{\circ}\text{S}$ ,  $155^{\circ}\text{W}$ ). Overall, model-data comparisons at this particular location show that RMSD values are 21, 22 and 26 m for buoy vs. NCOM, MODAS and climatology respectively, and

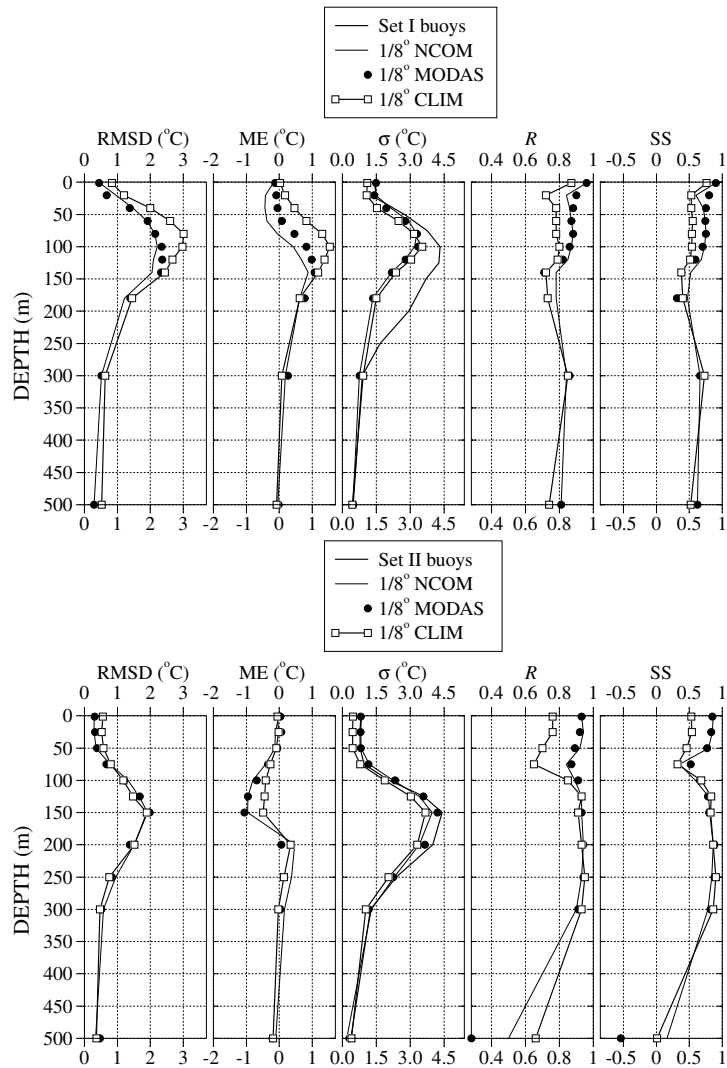


Fig. 7. Variations of RMSD, ME,  $\sigma$ ,  $R$  and  $SS$  values with depth from surface to 500 m below the sea surface at all buoy locations. The averaged statistical results for NCOM, MODAS and MODAS climatology are obtained combining subsurface temperatures from all locations. Note that the statistics is with respect to buoy values as explained in the text. Calculations were performed for set I and set II buoys, separately, as explained in the text.

corresponding  $SS$  values are 0.33, 0.27 and 0.05, demonstrating NCOM success in predicting MLD at this particular location.

#### 4.4. Salinity

Another model-data comparison for NCOM includes SSS and subsurface salinities. Daily salinity data from buoys are rather limited in comparison to SST and subsurface temperatures. Only a



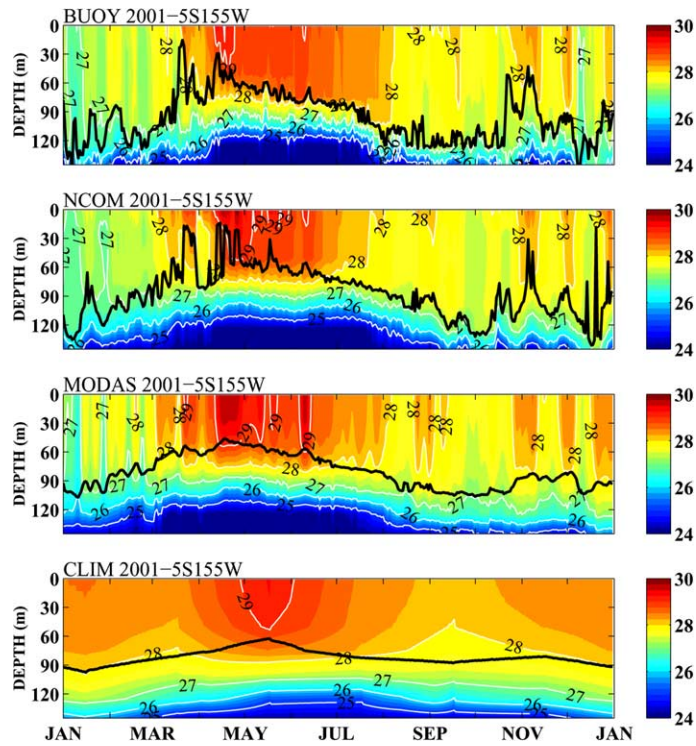


Fig. 8. Spatial daily MLD variability (thick black line) superimposed on daily subsurface temperatures ( $^{\circ}\text{C}$ ) obtained from buoy, NCOM and MODAS and MODAS climatology at a TAO buoy, ( $5^{\circ}\text{S}$ ,  $155^{\circ}\text{W}$ ), located in the central Pacific Ocean in 2001. Kara et al. (2000a) provides details of MLD calculations presented in this paper.

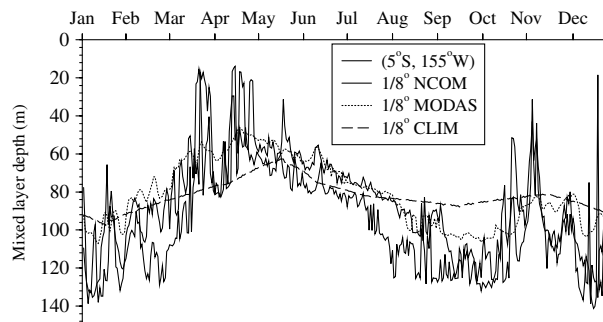


Fig. 9. Daily MLD time series obtained from buoy, NCOM and MODAS at ( $5^{\circ}\text{S}$ ,  $155^{\circ}\text{W}$ ). ME values between buoy vs. NCOM, MODAS and MODAS climatology are  $-9$ ,  $-14$  and  $-13$  m, and  $R$  values are 0.74, 0.77 and 0.69, respectively.

few TAO and PIRATA buoys routinely provide daily salinity measurements. Quality control methods for buoy salinity measurements included application of both pre-deployment, post-recovery calibrations and stability analysis among sensors. After correction, salinity data are believed to be accurate to within 0.02 psu. Technical details of buoy salinity measurements and

sampling procedures can be found in Freitag et al. (1999). For the model intercomparisons a few data voids are filled and no smoothing is applied to original buoy values. Daily SSS and subsurface salinities were also obtained from NCOM at the buoy locations. Note that NCOM does not assimilate any salinity data, but there is a weak relaxation to MODAS salinity as mentioned in Section 3.

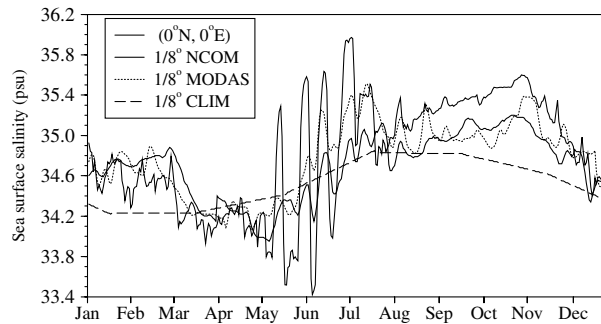


Fig. 10. Daily SSS time series obtained from buoy, NCOM and MODAS at (0°N, 0°E). Accuracy of salinities reported from the buoy is 0.02 psu. Note that global NCOM relaxes 1/8° MODAS SSS. Annual ME values between buoy vs. NCOM, MODAS and climatology are  $-0.13$ ,  $-0.04$  and  $-0.29$  psu, and  $R$  values are 0.53, 0.64 and 0.13, respectively.

Table 4

A list of daily sea surface salinity (SSS) and subsurface salinity availability from TAO and PIRATA buoys used for validating NCOM salinities in 2001

| Location      | ME values (Buoy vs. NCOM) |       |       |       | ME values (Buoy vs. MODAS) |       |       |       |
|---------------|---------------------------|-------|-------|-------|----------------------------|-------|-------|-------|
|               | SSS                       | 20 m  | 40 m  | 120 m | SSS                        | 20 m  | 40 m  | 120 m |
| (0°N, 00°E)   | -0.13                     | -     | -0.24 | -0.03 | -0.04                      | -     | -0.31 | -0.04 |
| (0°N, 035°W)  | -                         | 0.04  | 0.03  | -0.13 | -                          | -0.05 | -0.06 | -0.12 |
| (0°N, 110°W)  | -0.07                     | -     | -     | -     | -0.09                      | -     | -     | -     |
| (0°N, 125°W)  | 0.03                      | -     | -     | -     | 0.01                       | -     | -     | -     |
| (0°N, 140°W)  | -0.03                     | -     | -     | -     | -0.06                      | -     | -     | -     |
| (0°N, 155°W)  | -0.19                     | -     | -     | -     | -0.22                      | -     | -     | -     |
| (0°N, 170°W)  | -0.18                     | -     | -     | -     | -0.21                      | -     | -     | -     |
| (2°N, 140°W)  | -0.22                     | -     | -     | -     | -0.26                      | -     | -     | -     |
| (2°N, 165°E)  | -0.04                     | -     | -     | -     | -0.15                      | -     | -     | -     |
| (2°S, 095°W)  | -                         | -0.20 | -0.13 | -     | -                          | -0.29 | -0.17 | -     |
| (4°N, 038°W)  | 0.04                      | 0.02  | -     | 0.04  | -0.04                      | 0.04  | -     | 0.12  |
| (5°N, 095°W)  | 0.26                      | -     | -     | -     | 0.14                       | -     | -     | -     |
| (5°N, 140°W)  | 0.05                      | -     | -     | -     | -0.08                      | -     | -     | -     |
| (5°S, 140°W)  | 0.02                      | -     | -     | -     | 0.08                       | -     | -     | -     |
| (6°S, 010°W)  | -                         | -0.19 | -0.13 | 0.15  | -                          | -0.19 | -0.12 | 0.19  |
| (8°N, 038°W)  | -                         | -0.09 | 0.04  | 0.16  | -                          | 0.01  | 0.03  | 0.28  |
| (8°N, 095°W)  | 0.13                      | 0.11  | -0.01 | -     | 0.01                       | 0.06  | -0.14 | -     |
| (15°N, 038°W) | -0.19                     | -0.17 | 0.03  | -0.30 | -0.19                      | -0.14 | 0.08  | -0.24 |

Subsurface salinity data are available at 20, 40 and 120 m.

Time series of SSS obtained from buoy, NCOM and MODAS at (0°N, 0°E) in the equatorial Atlantic is seen in Fig. 10. Also included is the climatological MODAS SSS time series. While NCOM closely follows MODAS, neither NCOM nor MODAS is able to get sudden jumps in buoy SSS from May to June in 2001. MODAS seems to perform better than NCOM during this time period. One reason for the NCOM failure in predicting SSS is due to the weak salinity relaxation weights. It is also noted that there are currently no evaporation-precipitation effects taken into account in the simulations presented here. Overall, RMSD values at (0°N, 0°E) are 0.38, 0.33 and 0.52 psu for buoy vs. NCOM, MODAS and climatology respectively. These large RMSD values are due to large standard deviations (0.56, 0.33, 0.36 and 0.23 psu for buoy, NCOM, MODAS and climatological SSS, respectively). However, the skill values clearly reveals that NCOM is able to predict SSS with reasonable accuracy. SS values between buoy vs. NCOM, MODAS, and climatology are 0.53, 0.64 and 0.13. Both NCOM and MODAS SSS are better than climatological SSS.

Unlike SST and subsurface temperature, no median error statistics for salinity intercomparisons are calculated due to limited SSS and subsurface data. However, ME values at each location are provided in Table 4 for general information about accuracies of NCOM and MODAS salinities. Relatively small annual mean salinity bias is evident between buoy vs. NCOM and MODAS values for SSS and subsurface salinities.

## 5. Summary and conclusions

A 1/8° global version of the Navy Coastal Ocean Model (NCOM) is validated using extensive observational data sets. The model has both  $\sigma$ - and  $z$ -level coordinates, allowing the use of  $\sigma$ -coordinates near the surface to take up changes in surface elevation and in the shallow water, and the use of  $z$ -level coordinates in the steep shelf-break region. The simulations use 6-hourly atmospheric forcing from the Navy Operational Global Atmospheric Prediction System (NOGAPS). To measure the effectiveness of NCOM in predicting upper-ocean quantities, many buoys from the Tropical Atmosphere-Ocean (TAO) array in the equatorial Pacific, the Pilot Research Moored Array (PIRATA) in the equatorial Atlantic, and the National Oceanic Data Center (NODC) buoys located in coastal and open ocean areas are used. All the model-data comparisons presented in this paper include upper ocean quantities, such as SST, SSS, MLD, subsurface temperatures, and subsurface salinities. Additional model-data comparisons involving the eddy kinetic energy are also performed to determine performance of the model on large-scales.

Overall the model shows reasonable accuracy over a series of studies designed to test ability to represent upper ocean conditions and circulation. None of the validation data were assimilated into global NCOM directly or indirectly prior to their use for validation, maintaining their unambiguous independence for validation purposes. Global NCOM results in high latitudes are likely to be deficient (see figure 1c) for two reasons: poor or missing high-latitude results in NLOM and absence of an ice model and/or adequate ice treatment. Global NLOM is sub-global, excluding high-latitude regions, and MCSST observations are often sparse in the high latitudes as well, so the quality of MODAS SST-only synthetics at these latitudes is likely to be lower as well. Proposed solutions to these deficiencies are to add a coupled ice model, adding a real-time ice mask

using satellite-derived ice products, and blending in MODAS2D altimetry with NLOM to extend altimeter data to higher latitudes.

Skill in predicting SST is expected to be improved by a combination of factors. Comparisons of SST forecasts with unassimilated MCSSTs demonstrate problems in the SST immediately adjacent to land areas (now discussed here). The suggested source is bleeding of land values for heat flux and wind stress into ocean regions due to using winds not on the atmospheric native grid with an applied native atmospheric grid land mask. The solution proposed is to acquire operational fields on the native grid, apply the native grid land mask, and then regrid for ocean model forcing. Problems in SST in the equatorial Pacific warm pool in particular and an overall slight cold bias in SST forecasts has multiple solutions which must be tested in combination with the shallow bias in MLD in the equatorial regions. One solution is to modify the ocean attenuation for solar radiation from a clear-water setting to a setting derived from an available climatology of attenuation coefficient. This will tend to transfer more solar radiation to the surface and less to the deeper regions, tending to offset the bias seen in the eastern Pacific (Type I) profiles. However this will tend to increase the shallow bias in MLD, so we will also test modifications of the mixing scheme as well.

Validation of the first generation global NCOM system provides a baseline assessment of its capabilities and offers guidance for future development in preparation for its transition to operations at Naval Oceanographic Office (NAVOCEANO). As implemented, the model has the capability to provide daily hindcasts, analyses and three to five day forecasts on the operational computer resources and within the present time constraints.

The initial interannual validation of global NCOM assists in assessing its present performance and in indicating directions for improvement. Refinements to the initial global system include improved topography, addition of global river inflow (Barron and Smedstad, 2002) and upgrades to the data assimilation. Additional evaluations are collaborative efforts with more geographically focused interests and expertise. Through the efforts of many we hope to be able to better quantify regional confidence in the global NCOM analyses and forecasts, identify aspects of the system which are ripe for improvement, and verify the impact of model modifications on simulation results.

## Acknowledgements

The numerical simulations were performed under the Department of Defense High Performance Computing Modernization Program, on a IBM SP3 at the Naval Oceanographic Office, Stennis Space Center, Mississippi. We appreciate the input from Harley Hurlburt of Naval Research Laboratory (NRL) for his expertise on ocean modeling. Dong Ko at NRL provided the model grid generation and bathymetry data support, and Alan Wallcraft of NRL transformed the model code into its efficiently scalable form. Bill Schmitz (WHOI emeritus) offered valuable advice on the validation data. Additional thanks go to the National Data Buoy Center (NDBC) and M. McPhaden of the Tropical Ocean Array (TAO) project office for making daily SST and subsurface temperature data available for the model intercomparisons. Contributions to this work were funded as part of the NRL 6.4. Large-scale Models, 6.4 Ocean Data Assimilation and the 6.4 Small Scale Oceanography projects, managed by the Space and Naval Warfare Systems

Command under program element 0603207N. It received additional funding from the 6.1 Dynamics of Low latitude Western Boundary Currents project funded by the Office of Naval Research (ONR) under program element 601153N. This is contribution NRL/JA/7320/04/007 and has been approved for public release.

### Appendix A. A buoy locations

A list of TAO, PIRATA and NODC buoys which contain daily-averaged SST data used for NCOM SST intercomparisons in 2001 is provided. Water depths at buoy locations are also given. It should be noted that daily averages are constructed from hourly SST values.

| Buoy | Location (Lat, Lon) | Depth (m) | Buoy | Location (Lat, Lon) | Depth (m) |
|------|---------------------|-----------|------|---------------------|-----------|
| TAO  | (0°N, 140°W)        | 4359      | NODC | (17°N, 153°W)       | 5303      |
| TAO  | (0°N, 155°W)        | 4647      | NODC | (17°N, 158°W)       | 5002      |
| TAO  | (0°N, 170°W)        | 5616      | NODC | (19°N, 161°W)       | 4943      |
| TAO  | (2°N, 125°W)        | 4745      | NODC | (23°N, 162°W)       | 3257      |
| TAO  | (2°N, 140°W)        | 4387      | NODC | (26°N, 086°W)       | 3164      |
| TAO  | (2°N, 156°E)        | 2594      | NODC | (26°N, 090°W)       | 3246      |
| TAO  | (2°N, 165°W)        | 4183      | NODC | (27°N, 097°W)       | 78        |
| TAO  | (2°N, 170°W)        | 5408      | NODC | (28°N, 095°W)       | 82        |
| TAO  | (2°N, 180°W)        | 5477      | NODC | (29°N, 079°W)       | 841       |
| TAO  | (2°S, 125°W)        | 4751      | NODC | (29°N, 080°W)       | 42        |
| TAO  | (2°S, 140°W)        | 4320      | NODC | (29°N, 085°W)       | 53        |
| TAO  | (2°S, 180°W)        | 5353      | NODC | (29°N, 086°W)       | 283       |
| TAO  | (5°N, 095°W)        | 3577      | NODC | (29°N, 088°W)       | 237       |
| TAO  | (5°N, 125°W)        | 4395      | NODC | (29°N, 094°W)       | 15        |
| TAO  | (5°N, 140°W)        | 4490      | NODC | (32°N, 120°W)       | 1393      |
| TAO  | (5°N, 155°W)        | 4597      | NODC | (33°N, 079°W)       | 36        |
| TAO  | (5°N, 156°E)        | 3607      | NODC | (34°N, 119°W)       | 859       |
| TAO  | (5°N, 170°W)        | 5821      | NODC | (34°N, 120°W)       | 417       |
| TAO  | (5°N, 180°W)        | 5680      | NODC | (35°N, 073°W)       | 4389      |
| TAO  | (5°S, 110°W)        | 3605      | NODC | (35°N, 121°W)       | 185       |
| TAO  | (5°S, 125°W)        | 4561      | NODC | (36°N, 122°W)       | 1111      |
| TAO  | (5°S, 140°W)        | 4359      | NODC | (37°N, 075°W)       | 47        |
| TAO  | (5°S, 155°W)        | 5014      | NODC | (37°N, 122°W)       | 1920      |
| TAO  | (5°S, 156°E)        | 1528      | NODC | (38°N, 075°W)       | 28        |
| TAO  | (5°S, 170°W)        | 5418      | NODC | (38°N, 123°W)       | 122       |
| TAO  | (5°S, 180°W)        | 5664      | NODC | (38°N, 130°W)       | 4599      |
| TAO  | (8°N, 095°W)        | 3655      | NODC | (38°N, 071°W)       | 3163      |
| TAO  | (8°N, 125°W)        | 4659      | NODC | (39°N, 124°W)       | 264       |
| TAO  | (8°N, 155°W)        | 5249      | NODC | (40°N, 073°W)       | 40        |
| TAO  | (8°N, 156°E)        | 4920      | NODC | (40°N, 125°W)       | 82        |

**Appendix A** (continued)

| Buoy   | Location (Lat, Lon) | Depth (m) | Buoy | Location (Lat, Lon) | Depth (m) |
|--------|---------------------|-----------|------|---------------------|-----------|
| TAO    | (8°N, 170°W)        | 5553      | NODC | (41°N, 067°W)       | 88        |
| TAO    | (8°N, 180°W)        | 5955      | NODC | (41°N, 125°W)       | 274       |
| TAO    | (8°S, 110°W)        | 3465      | NODC | (41°N, 137°W)       | 4023      |
| TAO    | (8°S, 125°W)        | 4564      | NODC | (42°N, 071°W)       | 55        |
| TAO    | (8°S, 155°W)        | 5341      | NODC | (42°N, 124°W)       | 47        |
| TAO    | (8°S, 165°E)        | 3890      | NODC | (43°N, 130°W)       | 3420      |
| TAO    | (8°S, 170°W)        | 5371      | NODC | (44°N, 070°W)       | 18        |
| TAO    | (8°S, 180°W)        | 5535      | NODC | (46°N, 125°W)       | 128       |
| PIRATA | (0°N, 00°E)         | 4821      | NODC | (46°N, 131°W)       | 2779      |
| PIRATA | (4°N, 038°W)        | 4396      | NODC | (56°N, 148°W)       | 4206      |
| PIRATA | (8°N, 038°W)        | 4236      | NODC | (61°N, 147°W)       | 457       |
| PIRATA | (15°N, 038°W)       | 5762      |      |                     |           |

**References**

- Barron, C.N., Smedstad, L.F., 2002. Global river inflow within the Navy Coastal Ocean Model. In: Proceedings to Oceans 2002 MTS/IEEE Conference, 29–31 October 2002, pp. 1472–1479.
- Barron, C.N., Kara, A.B., Hurlburt, H.E., Rowley, C., Smedstad, L.F., 2004. Sea surface height predictions from the Global Navy Coastal Ocean Model (NCOM) during 1998–2001. *J. Atmos. Oceanic Technol.* 21, 1876–1894.
- Blumberg, A.F., Herring, H., 1987. Circulation modelling using orthogonal curvilinear coordinates. In: Nihoul, J., Jamart, B. (Eds.), *Three-dimensional models of marine and estuarine dynamics*. Elsevier Oceanography Series, 45, pp. 55–88.
- Blumberg, A.F., Mellor, G.L., 1987. A description of a three-dimensional coastal ocean circulation model. In: Heaps, N. (Ed.), *Three-dimensional Coastal Ocean Models*. American Geophysics Union, New York, 208p.
- Bretherton, F.P., Davis, R.E., Fandry, C.B., 1976. A technique for objective analysis and design of oceanographic experiments applied to MODE-73. *Deep Sea Res.* 23, 559–582.
- Brown, J.W., Brown, O.B., Evans, R.H., 1993. Calibration of Advanced Very High Resolution Radiometer infrared channels. *J. Geophys. Res.* 98, 18257–18268.
- Casey, K.S., Cornillon, P., 1999. A comparison of satellite and in situ based sea surface temperature climatologies. *J. Climate* 12, 1848–1863.
- Casey, K.S., Cornillon, P., 2001. Global and regional sea surface temperature trends. *J. Climate* 14, 3801–3818.
- D’Ortenzio, F., Marullo, S., Santoleri, R., 2001. Validation of AVHRR Pathfinder SST’s over the Mediterranean Sea. *Geophys. Res. Lett.* 27, 241–244.
- Fox, D.N., Barron, C.N., Games, M.R., Booda, M., Peggion, G., Gurley, J.V., 2002b. The Modular Ocean Data Analysis System. *Oceanography* 15, 22–28.
- Fox, D.N., Teague, W.J., Barron, C.N., Games, M.R., Lee, C.M., 2002a. The Modular Ocean Data Analysis System (MODAS). *J. Atmos. Ocean. Technol.* 19, 240–252.
- Freitag, H.P., Feng, Y., Mangum, L.J., McPhaden, M.J., Neander, J., Stratton, L.D., 1994. Calibration, procedures and instrumental accuracy estimates of TAO temperature, relative humidity and radiation measurements. NOAA Tech. Memo. ERL PMEL-104, 32 pp. [Available from PMEL, 7600 Sand Point Way, Seattle, WA 98115, USA].
- Freitag, H.P., McCarty, M.E., Nosse, C., Lukas, R., McPhaden, M.J., Cronin, M.F., 1999. COARE Seacat data: Calibrations and quality control procedures. NOAA Technical Memo. ERL PMEL-115, 89p [Available from PMEL, 7600 Sand Point Way, Seattle, WA 98115, USA].
- Hogan, T.F., Rosmond, T.E., 1991. The description of Navy Operational Global Atmospheric Prediction System’s Spectral Forecast Model. *Mon. Weather Rev.* 119, 1786–1815.

- Jacobs, G.A., Barron, C.N., Fox, D.N., Whitmer, K.R., Klingenberg, S., May, D., Blaha, J.P., 2002. Operational altimeter sea level products. *Oceanography* 15, 13–21.
- Kara, A.B., Hurlburt, H.E., Rochford, P.A., O'Brien, J.J., 2004. The impact of water turbidity on the interannual sea surface temperature simulations in a layered global ocean model. *J. Phys. Oceanogr.* 34, 345–359.
- Kara, A.B., Wallcraft, A.J., Hurlburt, H.E., 2003a. Climatological SST and MLD simulations from NLOM with an embedded mixed layer. *J. Atmos. Ocean. Technol.* 20, 1616–1632.
- Kara, A.B., Rochford, P.A., Hurlburt, H.E., 2003b. Mixed layer depth variability over the global ocean. *J. Geophys. Res.* 108, 3079.
- Kara, A.B., Rochford, P.A., Hurlburt, H.E., 2002. Air-sea flux estimates and the ENSO event. *Bound-Layer Meteor.* 103, 439–458.
- Kara, A.B., Rochford, P.A., Hurlburt, H.E., 2000a. An optimal definition for ocean mixed layer depth. *J. Geophys. Res.* 105, 16803–16821.
- Kara, A.B., Rochford, P.A., Hurlburt, H.E., 2000b. Mixed layer depth variability and barrier layer formation over the North Pacific Ocean. *J. Geophys. Res.* 105, 16783–16801.
- Kearns, E.J., Hanafin, J.A., Evans, R., Minnett, P.J., Brown, O.B., 2000. An independent assessment of Pathfinder AVHRR sea surface temperature accuracy using the MAERI. *Bull. Am. Meteor. Soc.* 81, 1525–1536.
- Martin, P.J., 2000. Description of the Navy Coastal Ocean Model Version 1.0. NRL Report No. NRL/FR/7322/00/9962, 45p (Available from NRL, Code 7322, Bldg. 1009, Stennis Space Center, MS 39529-5004, USA).
- Martin, P.J., Peggion, G., Yip, K.J., 1998. A comparison of several coastal ocean models. NRL Report No. NRL/FR/7322/97/9692, 96p (Available from NRL, Code 7322, Bldg. 1009, Stennis Space Center, MS 39529-5004, USA).
- McPhaden, M.J., Busalacchi, A.J., Cheney, R., Donguy, J.R., Gage, K.S., Halpern, D., Ji, M., Julian, P., Meyers, G., Mitchum, G.T., Niiler, P.P., Picaut, J., Reynolds, R.W., Smith, N., Takeuchi, K., 1998. The Tropical Ocean–Global Atmosphere (TOGA) observing system: a decade of progress. *J. Geophys. Res.* 103, 14169–14240.
- Millero, F.J., Poisson, A., 1981. International one-atmosphere equation of state of seawater. *Deep Sea Res. Part I* 28, 625–629.
- Millero, F.J., Chen, C.-T., Bradshaw, A., Schleicher, K., 1980. A new high pressure equation of state for seawater. *Deep Sea Res. Part I* 27, 255–264.
- Murphy, A.H., 1988. Skill scores based on the mean square error and their relationships to the correlation coefficient. *Mon. Weather Rev.* 116, 2417–2424.
- Murphy, A.H., Epstein, E.S., 1989. Skill scores and correlation coefficients in model verification. *Mon. Weather Rev.* 117, 572–581.
- Rhodes, R.C., Hurlburt, H.E., Wallcraft, A.J., Barron, C.N., Martin, P.J., Metzger, E.J., Shriver, J.F., Ko, D.S., Smedstad, O.M., Cross, S.L., Kara, A.B., 2002. Navy real-time global modeling systems. *Oceanography* 15, 29–43.
- Rosmond, T.E., Teixeira, J., Peng, M., Hogan, T.F., Pauley, R., 2002. Navy Operational Global Atmospheric Prediction System (NOGAPS): Forcing for ocean models. *Oceanography* 15, 99–108.
- Servain, J., Busalacchi, A.J., McPhaden, M.J., Moura, A.D., Reverdin, G., Vianna, M., Zebiak, S.E., 1998. A Pilot Research Moored Array in the Tropical Atlantic (PIRATA). *Bull. Am. Met. Soc.* 79, 2019–2031.
- Smedstad, O.M., Hurlburt, H.E., Metzger, E.J., Rhodes, R.C., Shriver, J.F., Wallcraft, A.J., Kara, A.B., 2003. An operational eddy-resolving 1/16° global ocean nowcast forecast system. *J. Mar. Res.* 40–41, 341–361.
- Stewart, T.R., 1990. A decomposition of the correlation coefficient and its use in analyzing forecasting skill. *Weather Forecast.* 5, 661–666.
- Wallcraft, A.J., Kara, A.B., Hurlburt, H.E., Rochford, P.A., 2003. The NRL Layered Global Ocean Model (NLOM) with an embedded mixed layer sub-model: Formulation and tuning. *J. Atmos. Ocean. Technol.* 20, 1601–1615.